Brain Stimulation 12 (2019) 267–274

Contents lists available at ScienceDirect

Brain Stimulation

journal homepage: http://www.journals.elsevier.com/brain-stimulation

Methods to monitor accurate and consistent electrode placements in conventional transcranial electrical stimulation

Aprinda Indahlastari*, Alejandro Albizu, Nicole R. Nissim, Kelsey R. Traeger, Andrew O'Shea, Adam J. Woods

Department of Clinical and Health Psychology, Department of Neuroscience, Center for Cognitive Aging and Memory, McKnight Brain Institute, University of Florida, Gainesville, FL, USA

ARTICLE INFO

Article history:
Received 18 September 2018
Received in revised form
23 October 2018
Accepted 24 October 2018
Available online 28 October 2018

Keywords:
tES
Electrode placements
Quality control
Electrode drift

ABSTRACT

Background: Inaccurate electrode placement and electrode drift during a transcranial electrical stimulation (tES) session have been shown to alter predicted field distributions in the brain and thus may contribute to a large variation in tES study outcomes. Currently, there is no objective and independent measure to quantify electrode placement accuracy/drift in tES clinical studies.

Objective/hypothesis: We proposed and tested novel methods to quantify accurate and consistent electrode placements in tES using models generated from a 3D scanner.

Methods: Accurate electrode placements were quantified as Discrepancy in eight tES participants by comparing landmark distances of physical electrode locations F3/F4 to their model counterparts. Distances in models were computed using curve and linear based methods. Variability of landmark locations in a single subject was computed for multiple stimulation sessions to determine consistent electrode placements across four experimenters.

Main results: We obtained an average of 0.4 cm in Discrepancy, which was within the placement accuracy/drift threshold (1 cm) for conventional tES electrodes (~35 cm^2) to achieve reliable tES sessions suggested in the literature. Averaged Variability was 5.2%, with F4 electrode location as the least consistent placement.

Conclusions: These methods provide objective feedback for experimenters on their performance in placing tES electrodes. Applications of these methods can be used to monitor electrode locations in tES studies of a larger cohort using F3/F4 montage and other conventional electrode arrangements. Future studies may include co-registering the landmark locations with imaging-derived head models to quantify the effects of electrode accuracy/drift on predicted field distributions in the brain.

© 2018 Elsevier Inc. All rights reserved.

Introduction

Transcranial electrical stimulation (tES) is a promising non-invasive neuromodulation technique that can affect brain functions [1–6]. In tES, a mild electrical current (e.g., 2 mA) is applied via two or more electrodes that are placed directly on the scalp. Conventional tES uses a pair of bicarbon pads (surface area ca. 35 cm^2) with one anode and one cathode as electrodes that are secured on the head using elastic straps. Saline soaked sponges encapsulating the electrodes, or other electrolytes e.g., conductive paste applied on the electrode surface, are used to minimize scalp sensations while providing good contacts for electrical stimulation [1]. Electrode configurations in tES are based on previously established methods to localize electrode position, such as the standard 10–20 EEG System [1]. The choices of different electrode montages used in tES are typically determined based on intended stimulation regions [1,7,8]. For instance, electrode montage F3/F4 is widely used in tES to target the left and right dorsolateral prefrontal cortex (DLPFC) to improve cognitive processes related to these regions, such as decision-making and working memory [1,9–11].

The number of empirical studies investigating tES effects in healthy and diseased population has been growing exponentially in the last decade, yet the efficacy and reproducibility of tES studies remain unsolved. Many clinical tES studies have used insufficient sample sizes to report significant stimulation effects, and thus

* Corresponding author. Department of Clinical and Health Psychology, University of Florida, Gainesville, FL, USA.
E-mail address: aprinda.indahlas@phhp.ufl.edu (A. Indahlastari).

https://doi.org/10.1016/j.brs.2018.10.016
1935-861X/© 2018 Elsevier Inc. All rights reserved.

reported tES effects could be under- or overestimated and subject to publication bias [12–14]. Additionally, a large variability in reported individual responses to tES suggested that using the same nominal electrode placements might not produce the same effects across individuals [15,16]. Current dose in the brain resulting from different combination of stimulation parameters such as current intensity, stimulation duration and electrode montage has been considered crucial in individual physiological responses caused by tES [1,17,18]. However, the actual stimulation current dose in individual brain structures cannot be measured *in-vivo* and thus making it difficult to validate and repeat observed outcomes. Therefore, current flow modeling studies using realistic human head models have been employed to predict current dose in the brain caused by tES [19–22] and validated against tES *in-vivo* studies in humans [23–27].

Electrode drift in tES has been shown to alter predicted current density and electrical field distributions in the brain [28–30]. Our previous finite element modeling study showed that a 5% drift in electrode positions involved in M1/SO and F3/F4 montages could significantly alter predicted electric field distributions caused by tES [28]. The 5% electrode drift was equivalent to 1–1.5 cm distance on average human heads, which was later suggested by Opitz et al. [31] as the threshold of electrode placement accuracy to achieve reliable stimulation sessions. Spatial correlations between the electric field for each electrode position and the computed electric field from target electrode location continued to decrease as the electrode was positioned further away from the target electrode location [31]. Implications of these findings suggested that electrode drift larger than 1 cm from the intended electrode positions of the same montage could significantly change the shape of field distribution and thus might alter stimulation current dose in targeted cortical regions. Therefore, ensuring accurate and consistent electrode placements might be key to achieve reliable and meaningful results in tES studies [28,29].

At present, there is no independent measure to objectively monitor accurate and consistent placements of tES electrodes. Electrode montages reported in previous tES studies are assumed to be in correct locations that are predetermined using the standard 10–20 EEG System or the neuronavigation system. While the Standard EEG 10–20 System is considered as an objective method, actual applications of head measurement procedure following this system may vary depending on the experimenters' experience and are subject to human error. Therefore, a lack of good practice in electrode placements can result in a seemingly small error that shifts electrode position with potentially significant impacts on outcomes [31]. Improper use of the elastic straps to hold the electrodes in place might also cause the electrodes to drift. These issues raise a concern of the importance in documenting electrode drift during tES sessions. Therefore, there is a need in quantification of electrode drift to ensure reliable electrode placements and can potentially serve as covariates related to variability in observed tES outcomes.

In this study, we proposed methods to quantify accuracy and consistency of conventional tES electrode placements. Individual electrode locations were identified as landmarks at the center of each electrode and converted to 3D models using a 3D scanner. Landmark distances in generated models were compared to physical measurements as a metric of electrode placement accuracy. The same landmark locations of the same subjects were then compared across multiple stimulation sessions to quantify electrode placement consistency. We applied the proposed methods in eight tES participants who underwent stimulation in F3/F4 configurations and obtained an average of 0.4 cm in electrode drift with 5.2% averaged variability in placement consistency. Methods presented in this study provide a simple tool to measure accurate and consistent electrode locations and can be used as quality control to monitor electrode placements in future tES studies.

Methods

A total of two phantom objects, two dummy subjects and eight tES participants were included to test landmark accuracy calculation. All landmark locations were annotated using green stickers with 6 mm in diameter and landmark distances were physically measured using a tape measurement. Marked objects were then scanned and converted into 3D models. Distances between the landmarks in generated models were calculated using curve and linear based methods. Our initial study outlining the accuracy metric tested in phantom and dummy subjects has been previously submitted as a conference proceeding [Indahlastari et al., 2018, *in prep*]. An additional metric to quantify landmark consistency was performed in two dummy subjects and eight tES participants. All experimental procedures involving tES participants reported in this study followed the protocols approved by the University of Florida Institutional Review Board. Details on data collection, model construction and landmark metrics computation are described in the following sections.

Validation experiments

A rectangular object (18 × 25 × 29 cm) with a flat surface and a spherical object (diameter ~66 cm) with smooth curvy surface were used as phantom objects. Eight and five landmark locations were arbitrarily chosen in rectangular and spherical phantom, respectively. The physical distances between selected pairs of landmarks as shown in Fig. 1 were measured and recorded. Five consecutive scans were performed on each phantom to generate five 3D models of each kind.

Head measurements following the 10–20 EEG System for F3/F4 montage were performed in two dummy subjects, Dummy A (male)

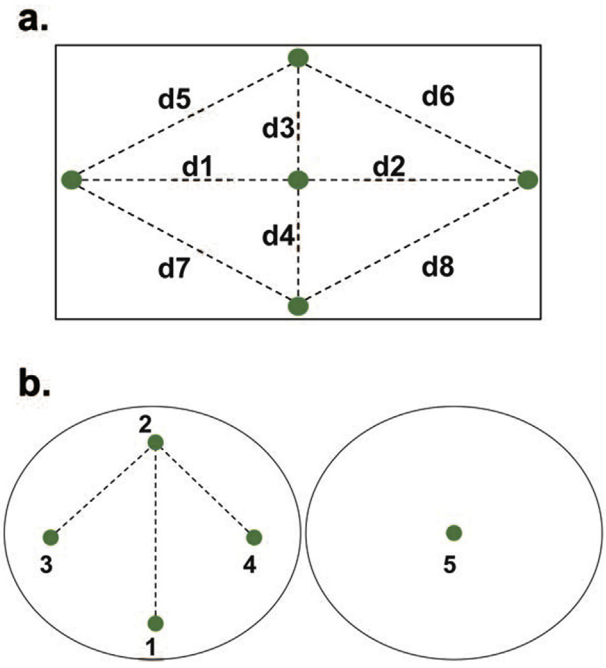

Fig. 1. Selected landmark locations in phantom objects. Individual landmarks are noted by green dots in a) rectangular and b) spherical phantom. (For interpretation of the references to color in this figure legend, the reader is referred to the Web version of this article.)

and Dummy B (female). Green stickers were placed on four landmark locations: Nasion, Fz, F3 and F4 before (PRE) and after (POST) electrode placements. Carbon rubber pad electrodes (5 × 5 cm) were inserted in saline soaked sponges (5 × 7 cm, thickness up to 1 cm) and placed on F3/F4 location such that the green stickers were centered in each electrode. *Direct* measurements defined as the shortest distances between green stickers on landmark Nasion-Fz, Fz-F3 and Fz-F4 were also recorded. Five consecutive scans were performed during PRE and POST to generate ten head models per subject.

tES participants

Head scans of eight tES participants in an active phase 2 and phase 3 clinical trial [32] were randomly selected to test the accuracy and consistency metric computation. A total of five males and three females (mean age 69.9, age range 65–77 years old) received either active or sham stimulation using F3/F4 montages with F4 as the anode and F3 as the cathode electrode site. Each stimulation session was administered as 2 mA direct current for 20 minutes in multiple consecutive days ranging from 10 to 19 days. Head measurements following the 10–20 EEG System were performed in each participant by study interventionists (E1-4) to place tES electrodes in F4 and F3 location. After securing the electrodes with a strap, green stickers were placed at Nasion, Fz, F4 and F3 location. Each participant was then scanned using a 3D scanner prior to stimulation. Details on subject demographic including stimulation days, the amount of hair surrounding landmark locations and study interventionists are summarized in Table 1.

Table 1
Details on selected eight tES participants for landmark accuracy and consistency calculation.

Subject	Gender	Stim. Length (days)	Hair near Landmarks	Interventionist
1	Female	10	Low	E1
2	Male	10	Low	E1
3	Female	10	High	E2
4	Female	10	High	E1
5	Male	18	High	E3
6	Male	19	Low	E3
7	Male	18	Low	E3
8	Male	19	Low	E4

Model construction

Upon placing green stickers on selected landmarks, each object was scanned using 3DSizeMe software and an external 3D scanner [TechMed 3D, Quebec City] mounted on an iPad Air 2 [Apple Inc., CA]. All scanned datasets were imported to MSoft software [TechMed 3D, Quebec City] for preprocessing steps prior to landmark distance calculation. Landmarks on the scanned objects that were not automatically detected in the software were generated manually. All processed landmarks in each model were exported into a text file for linear distance calculation. During the preprocessing steps, each head model orientation was normalized by following instructions in MSoft software. The normalized head models were then clipped using a bounding box spanning from chin to the head apex (z-axis), left to right ear (y-axis), and tip of the nose to the back of the head (x-axis). The vertices of the clipped head models were then exported into ASCII text file for consistency metric calculation.

Landmark accuracy metric

Landmark accuracy metric was defined as the discrepancy between actual landmark distances measured directly on objects ($Distance_{actual}$) and those computed in the generated 3D models of the objects ($Distance_{model}$), such that:

$$Discrepancy = Distance_{actual} - Distance_{model} \quad (1)$$

In phantom, the $Distance_{actual}$ was the shortest distance measured between two landmarks. In dummy subjects and tES participants, the $Distance_{actual}$ was the measured distance between the landmark Nasion-Fz (30% of Nasion-Inion distance), Fz-F3 (20% of preauricular points) and Fz-F4 (20% of preauricular points) according to the 10–20 EEG System. In dummy subjects, additional values for $Distance_{actual}$ were also obtained using *direct* measurements, which was the shortest distance measured between the two landmarks. Computed discrepancy values using these $Distance_{actual}$ values were then compared between PRE and POST to determine any effects from the electrode thickness on computed landmark accuracy. $Distance_{model}$ was calculated in generated 3D models by

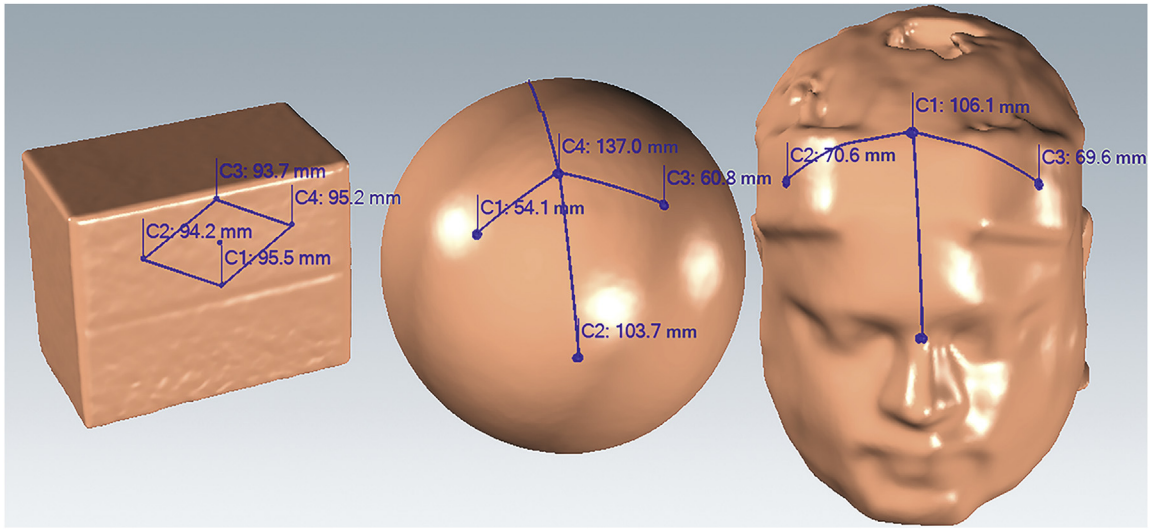

Fig. 2. Curve based method to measure landmark distances in generated models. Illustrations from left to right are computed landmark distances using MSoft in rectangular phantom, spherical phantom and Dummy A. Annotated values (C1-C4) in each model corresponding to landmark: d5-d8 in rectangular phantom, 1–4 in spherical phantom, and Nasion-Fz, Fz-F4, Fz-F3 in head models.

using two methods: curve based and linear based. Curve based methods utilized a measuring tool within MSoft GUI that included the surface curvature of the objects as shown in Fig. 2. Linear based methods used the Euclidean distance (D) formula to compute linear distance between landmark coordinates as follow:

$$D = \sqrt{(x - x_1)^2 + (y - y_1)^2 + (z - z_1)^2} \quad (2)$$

In-house MATLAB [MathWorks, MA] codes were used to sort landmark category (Nasion, Fz, F4 and F3) within the text files and compute linear distance of Nasion-Fz, Fz-F4 and Fz-F3.

Landmark consistency metric

To quantify the consistency of electrode placements across head scans of the same subjects that were collected in multiple days, we computed the variability of landmark location Nasion, Fz, F4 and F3 using the coefficient of variation formula such that:

$$\text{Variability} = \frac{\text{Std Dev}}{\sqrt{x^2 + y^2 + z^2}} \times 100\% \quad (3)$$

where Std Dev is the standard deviation of individual x,y, and z-coordinates of landmark locations across multiple days for each subject. Prior to Variability computation, preprocessed individual head models collected from multiple days were aligned by zeroing the xyz-coordinates according to the three chosen facial features i.e., the tip of the nose (x), the left ear (y) and the bottom of the chin (z).

Results

Computed Discrepancy values are summarized in Table 2, Figs. 3 and 5. Negative numbers of Discrepancy values indicated that the physical measurements ($\text{Distance}_{\text{actual}}$) in objects were smaller than computed distances in their modeled counterparts ($\text{Distance}_{\text{model}}$). The average preprocessing time for head models was 86 seconds. CB measurements in head models took 80 seconds to complete while LB measurements took less than 1 second per subject on average. Percentages shown in Figs. 4 and 6 are calculated Variability values of landmarks located in Nasion, Fz, F3 and F4.

Table 2
Computed Discrepancy in rectangular and spherical phantom objects. Physical measurements of landmark distances were recorded and compared to the same distances in models calculated using curve based (CB) and linear based (LB) methods. Absolute percentage differences (|PD|) between CB and LB were computed with respect to CB.

Rectangular Phantom			
DISTANCE	**DISCREPANCY**		
Actual (mm)	**CB (mm)**	**LB (mm)**	**|PD|(%)**
81	−0.72 ± 0.28	−0.72 ± 0.27	0.00
80	0.58 ± 0.37	0.6 ± 0.34	3.45
51	0.08 ± 0.26	0.08 ± 0.25	0.00
50.5	0.48 ± 0.24	0.49 ± 0.21	2.08
93	−1.8 ± 0.46	−1.79 ± 0.46	0.56
95	0.86 ± 0.3	0.87 ± 0.28	1.16
95	−0.76 ± 0.24	−0.76 ± 0.25	0.00
95	−0.52 ± 0.31	−0.51 ± 0.32	1.92
Average	−0.23 ± 0.31	−0.22 ± 0.3	0.53
Spherical Phantom			
Actual (mm)	**CB (mm)**	**LB (mm)**	**|PD|(%)**
103	−1.02 ± 1.68	3.35 ± 1.42	4.37
59.5	1.36 ± 3.71	2.3 ± 3.56	0.94
63	1.98 ± 2.34	2.78 ± 2.23	0.80
137	0.14 ± 3.64	9.76 ± 2.72	9.62
242	1.64 ± 3.5	51.55 ± 1.6	49.91
Average	0.82 + 13.95	2.97 + 2.31	13.13

Phantom objects

Table 2 shows actual measured distances and Discrepancy values computed in the rectangular and spherical phantom. Discrepancy values computed in the rectangular phantom had an average of −0.23 ± 0.31 mm for curve based (CB) and −0.22 ± 0.3 for linear based (LB) methods. The average of absolute percentage differences (|PD|) between CB and LB measurements in rectangular phantom was 0.53%. In spherical phantom, the average Discrepancy values were 0.82 ± 2.97 mm for CB and 13.95 ± 2.31 mm for LB calculations. Computed |PD| between CB and LB measurements were up to 9.62% for distances of 137 mm or less, with the largest |PD| of 49.91% for landmark distance 242 mm apart.

Dummy subjects

Fig. 3 shows computed Discrepancy in dummy subjects using actual distances obtained from following the 10–20 EEG System and using *direct* measurements. Absolute Discrepancy values for actual distances following the 10–20 EEG System (Fig. 3a) were up to 12.38 mm and 7.14 mm for CB and LB methods, respectively. Calculated Discrepancy using *direct* measurements before and after electrode placements in both subjects is shown in Fig. 3b with an average Discrepancy of 0.54 mm.

Calculated Variability values corresponded to landmark placements in five consecutive 3D scans are summarized in Fig. 4. Overall, Dummy A had smaller Variability values compared to Dummy B for all landmark locations. The average Variability was 1.9% and 2.9% for Dummy A and B, respectively. Landmark placements at the Nasion location were the most consistent with averaged Variability of 1.9% (PRE) and 2.3% (POST).

tES participants

Computed Discrepancy of landmark distances Nasion-Fz, Fz-F4 and Fz-F3 in eight tES participants is shown in Fig. 5. Absolute Discrepancy values were in the range of 0.02–13.26 mm for CB and 0.01–7.72 mm for LB methods. Overall, CB method produced smaller Discrepancy values than LB in subjects with less hair obstruction near the landmarks. The smallest absolute values of averaged Discrepancy were 0.10 mm for CB (Subject 2) and 0.30 mm for LB calculation (Subject 4). The largest absolute CB Discrepancy was 13.26 mm found in Subject 3 while the largest absolute LB Discrepancy was 7.72 mm in Subject 6.

Fig. 6 summarizes computed Variability in individual tES participants. The range of computed Variability was from 3.9% (Subject 4) to 9.8% (Subject 1). Landmark locations were the most consistent for Nasion placement (ca. 3.8%) and the least consistent for F4 placement (ca. 6.8%). The average Variability for all four landmark placements produced by Interventionist E1 to E4 was 5.4%, 4.9%, 5.4% and 4.0%, respectively.

Discussion

This study presented and tested novel methods to estimate the accuracy and consistency of landmark locations associated with tES electrode placements. Physical measurements of landmark distances in objects and subjects were compared to the same distances computed in their 3D model counterparts. Landmark distances in models were computed using curve based (CB) and linear based

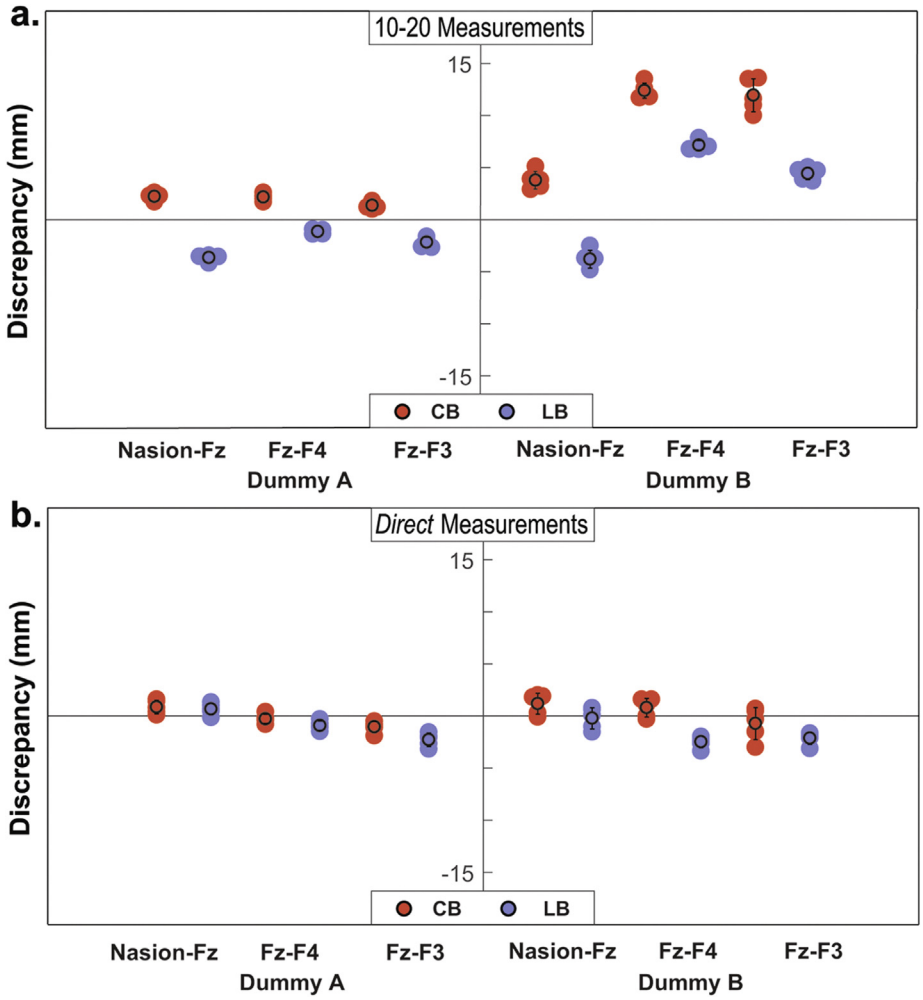

Fig. 3. Computed Discrepancy in two dummy subjects. Landmark distances Nasion-Fz, Fz-F4 and Fz-F3 were compared between those measured in subjects and in models. Actual distances were computed using a) the 10–20 EEG System and b) *direct* measurements (the shortest distance between two landmarks).

(LB) measurements. The proposed accuracy and consistency methods were tested in eight tES participants that underwent multiple stimulation sessions using an F3/F4 montage. The context of our findings, study limitations and future direction are discussed in the sections below.

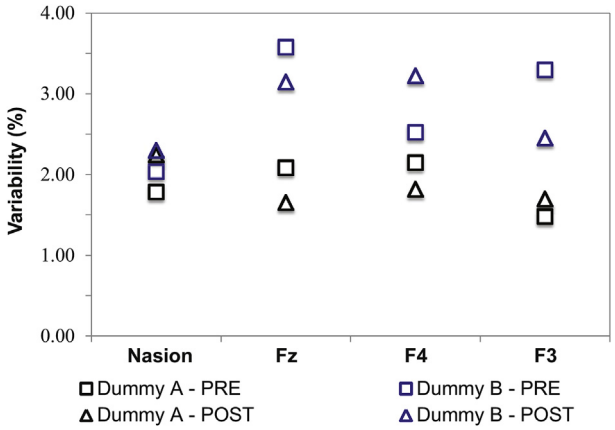

Fig. 4. Computed Variability in two dummy subjects. Individual percentage values represented five consecutive 3D scans of landmarks before (PRE) and after (POST) electrode placements.

Model validation

Results from phantoms and dummy subjects indicated that landmark locations in generated models were good representations of their actual locations. For instance, the average Discrepancy in the rectangular phantom (ca. −0.23 mm) suggested that the difference between landmark locations in objects and their model counterparts were negligible. Therefore, comparisons made between landmark distances computed in models and the actual measured distances in objects were considered valid. Further, landmark distance Fz-F4 and Fz-F3 in head models were computed based on the green stickers placed on F4 and F3 electrodes, and compared to markings on the scalp prior to electrode placements. This method of comparison might raise a concern of any unknown effect of electrode thickness on computed Discrepancy. We performed *direct* measurements in dummy subjects to quantify this effect and obtained an average Discrepancy of 0.54 mm, which was ~1% of the electrode's length. Therefore, we considered electrode thickness to have a negligible effect on accuracy metric computation and thus verified the Discrepancy values computed between model and actual measurements.

The 3D scanner used in this study might produce inconsistent images and, in turns, could alter the rendering of landmark locations in scanned objects affecting computed landmark accuracy.

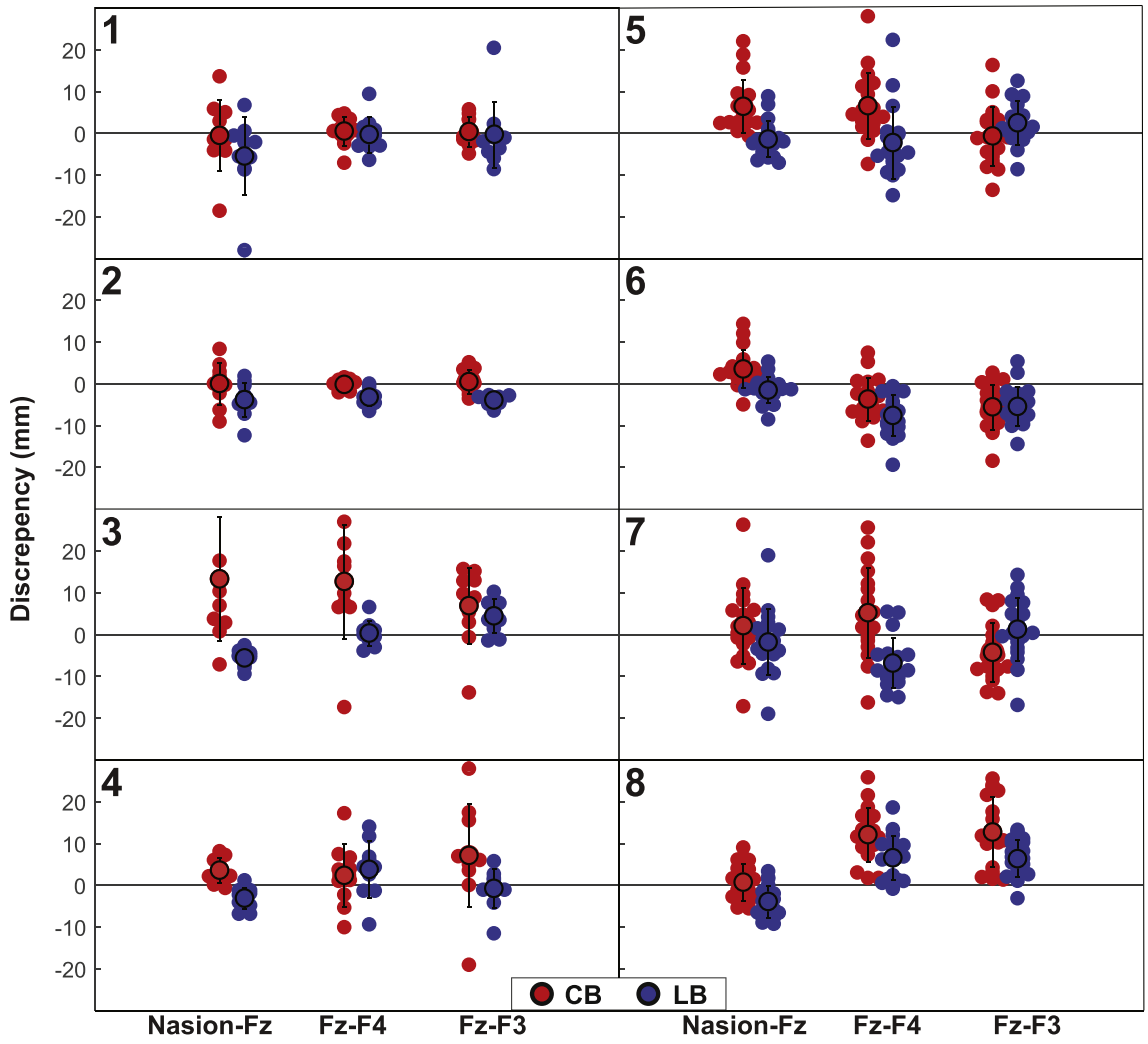

Fig. 5. Computed Discrepancy as a measure of electrode placement accuracy in eight tES participants. Positive and negative values of Discrepancy indicating whether the distances measured in models were larger or smaller than physical measurements, respectively. Landmark distances in generated head models were calculated using curve based (CB) and linear based (LB) methods.

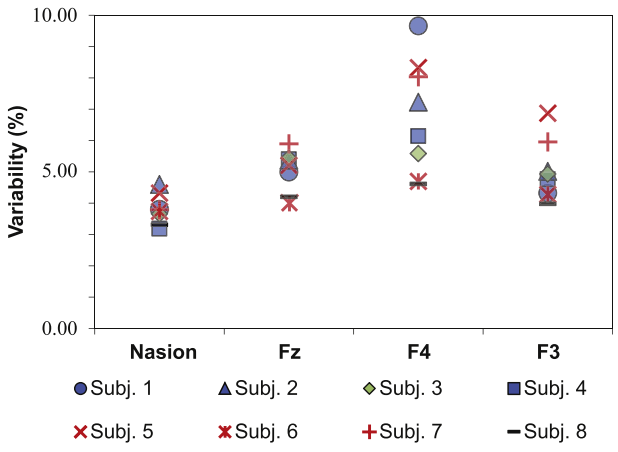

Fig. 6. Landmark Variability computed in each tES participant. Percentage values corresponding to individual subjects are color-coded based on the study interventionist E1 (blue), E2 (green), E3 (red) and E4 (black). (For interpretation of the references to color in this figure legend, the reader is referred to the Web version of this article.)

Five consecutive scans in each dummy subject were acquired to test the consistency of landmark positions captured by the scanner. Our findings showed that computed Variability in these five scans were averaged at 2.9% and thus indicating that the 3D scanner used for this study was capable to produce reliable images within 3% Variability.

Curve based versus linear based measurements

Using LB methods to estimate landmark distances on a curved surface was limited to the spread of landmark locations, and thus the appropriate usage of LB methods is determined based on the distance spanned between the electrodes. As expected, we obtained larger absolute percentage differences between landmark distances computed using CB and LB, as the two landmark locations were further apart (Table 2). We tested the accuracy metric on landmarks associated with F3/F4 montage and the furthest landmark location for this montage was 108 mm apart. Calculated absolute percentage differences in the spherical phantom were 4.37% and 9.62% for landmark distances of 103 mm and 137 mm apart. Assuming that the head surface was fairly smooth, computed Discrepancy values using LB and CB in head models should differ by

5–10%. This observation indicated that either CB or LB methods was sufficient to use and produced up to 10% difference in computing Discrepancy associated with F3/F4 montage, or with other montages involving electrode locations within 137 mm apart.

While, intuitively, LB methods are expected to produce less accurate measurements than CB methods on curved surfaces (e.g., human heads), our results indicated that preferred applications of either CB or LB measurements in head models would depend on hair presence surrounding the landmarks. The scanned images of the head included subjects' hair and thus any hair surrounding the landmarks were rendered as rough terrains at the surface of generated 3D models. Therefore, CB measurements in head models produced more accurate distances than LB when applied on smoother head surface i.e., with minimal hair obstruction nearby the landmark locations. For instance, Subject 2 was bald and computed Discrepancy on this subject was the smallest for CB measurements (ca. −0.10 mm). On the contrary, landmark distances in models computed using LB methods were more accurate in subjects with more hair surrounding the landmarks such as seen in Subject 3. Therefore, LB methods might be more appropriate to use than CB in head models with more hair presence in between the landmark locations.

LB method produced more consistent Discrepancy values and was faster to complete compared to CB measurement process. The standard deviations of computed Discrepancy in the spherical phantom, dummy subjects and tES participants were mostly larger for CB measurements, indicating that computed Discrepancy using CB method was highly variable. The procedure to perform CB measurements required manual labor and thus might contribute to variation of measured CB values. Further, LB measurement process can be automated for batch processing, which is useful for monitoring electrode placements in tES clinical studies with larger cohort, such as in our ongoing phase 3 tES ACT trial [32].

Applications in quality control for electrode placements

Computed Discrepancy in landmark distances of individual head models can be used as a feedback tool for experimenters on their performance in tES electrode placements. In this study, the landmark locations in tES participants were selected based on electrode placement F3/F4. Large values in computed Discrepancy suggested that landmark locations in generated head models did not align with their actual locations that were determined using the 10–20 EEG System. Since the landmarks were placed at the center of individual electrodes, larger Discrepancy values in landmark locations corresponded to less accurate placements of electrodes. Therefore, our proposed methods offer an accuracy metric calculation that can be completed after each stimulation session and serve as quantitative feedback to study interventionists. Computed Discrepancy values may be used to keep track all electrode positions involved in multiple stimulation sessions, and serve as covariates for future data analyses to determine potential effects of varying electrode locations on stimulation outcomes.

Calculated Variability values indicated whether electrode placements performed by experimenters were consistent across multiple stimulation sessions and thus can be used to evaluate existing study protocols. Electrode placements in eight tES participants were performed by different study interventionists (E1-4) as listed in Table 1. Comparisons of Variability results between interventionists with the same number of subjects reflected their individual performances in placing the landmarks. For instance, interventionist E3 was less consistent (5.7%) compared to E1 (4.7%) when placing F3 electrode as shown in Fig. 6. As expected, all interventionists were the most consistent in placing the landmark at Nasion location (ca. 3.8%) because of an anatomical landmark (nose bridge) associated with this location. On the contrary, F4 placements were the least consistent (ca. 6.8%) and had the most variation across interventionists. This large variation could be caused by the order of electrode insertion under the strap. According to the study protocol, the anode electrode (F4) was secured first under the strap followed by securing the cathode electrode (F3). Therefore, the F4 electrode might have had shifted underneath the strap during the placement of F3 electrode. This finding suggested that extra caution is needed while securing multiple electrodes underneath the strap, and that the electrodes may need readjustment prior to the start of stimulation to ensure correct stimulation sites.

Study limitations and future direction

Computed Discrepancy to estimate electrode placement accuracy was mainly leveraging the assumption that the head measurements were done correctly. Individual head measurements reported in this study were based on the standard 10–20 EEG System and performed by different study interventionists. While a standardized method was used, other factors such as human error could introduce a variation in obtaining landmark locations. Therefore, our accuracy metric was limited to the discretion of correct head measurements and thus ignored possible human error during the physical measurement of the head. Generating ideal electrode locations of the 10–20 EEG System in individual head models derived from imaging data might provide more accurate reference points for landmark locations, but would represent a significant increase in study requirements and study cost.

Our proposed methods were tested in a single montage of conventional tES electrodes and did not include other types of tES electrodes and montages. We expect our proposed methods to be applicable in other electrode types and montages as long as landmark locations are visible in the scanned images. However, annotating the landmark such as using green stickers may be challenging depending on the surface condition of the electrode. For instance, any excess gel use with multi-array tES electrodes may cause the stickers difficult to adhere, and thus will require an alternative way to mark the electrodes. Further, our findings indicated that using LB methods were limited to electrode montages within 137 mm apart. Multi-array tES electrode configurations typically involve smaller distances in between the electrode locations [22] and thus either CB or LB methods are good candidates to use for these electrode arrangements.

Despite CB and LB measurement methods, we recognize the need of using a more accurate distance calculation method that includes the curvature of the head without the rendering of subject's hair. The distance measurement techniques used in this study demonstrated a quick way to compute the distances in models using unaltered rendering of the head scans. Other techniques that generate smoother head models without the presence of hair can be explored to produce more accurate landmark distance calculations in models. For instance, mapping landmark coordinates on realistic head models generated from individual T1 images to compute landmark distances for the accuracy metric.

Our proposed methods did not account for electrode orientation e.g., to detect possible rotations in multiple electrode placements of the same subjects. Electrode orientation during tES dictates the shape of stimulation contact area and thus any discrepancy in electrode orientation may alter the pattern of stimulated current flow to the brain. In this study, we only used a single marker that was centralized in each electrode to compute the accuracy and consistency metric. Therefore, our results were limited to translational error at the center of the electrodes and neglecting any potential discrepancy caused by variations of electrode orientation. However, our methods can be extended to include multiple

markers for each electrode. These markers can be placed sparsely along the electrode's edge to capture the orientation of individual electrode placements. An additional metric calculation to quantify the degree of rotation in each electrode is then required to carefully track any changes in electrode orientation across multiple stimulation sessions.

Conclusion

Clinical studies involving tES have been growing exponentially, yet reproducibility of these studies remains a challenge. Reported individual responses to stimulation effects of tES have varied, including stimulation sessions that used the same electrode montages. Previous computational studies have shown that electrode drift within the same montage can alter field distributions in the brain and thus may affect observed tES outcomes. At present, there is no standardized protocol to monitor tES electrode locations and thus making it difficult to ensure correct electrode placements across tES studies. In this study, we proposed novel methods to estimate electrode location accuracy and consistency using head models generated from a 3D scanner. We tested our methods in eight tES participants underwent multiple days of stimulation in F3/F4 montage. Our preliminary results showed that the average accuracy in electrode placements across all participants was 0.4 cm and up to 1.36 ± 0.3 cm in one participant, which was slightly greater than the recommended threshold (1 cm) of electrode drift to conduct reliable tES studies [28,31]. Findings from this study can be coupled with current flow modeling to quantify any changes in predicted current density distributions caused by computed electrode drift. Applications of these methods can be used to monitor electrode placements in tES studies involving F3/F4 montages and expanded to include other electrode montages. Future studies may include a larger cohort and refinements of landmark distance measurements in generated head models using imaging data.

Author declaration

The authors report no conflicts of interest.

Acknowledgements

This work was supported in part by the National Institute of Aging/National Institutes of Health (K01AG050707, R01AG054077).

References

[1] Woods AJ, Antal A, Bikson M, Boggio PS, Brunoni AR, Celnik P, et al. A technical guide to tDCS, and related non-invasive brain stimulation tools. Clin Neurophysiol 2016;127(2):1031–48.
[2] Bikson M, Grossman P, Thomas C, Zannou AL, Jiang J, Adnan T, et al. Safety of transcranial direct current stimulation: evidence based update 2016. Brain Stimul 2016;9(5):641–61.
[3] Brunoni AR, Moffa AH, Sampaio-Junior B, Galvez V, Loo CK. Treatment-emergent mania/hypomania during antidepressant treatment with transcranial direct current stimulation (tDCS): a systematic review and meta-analysis. Brain Stimul 2017;10(2):260–2.
[4] Nikolin S, Huggins C, Martin D, Alonzo A, Loo CK. Safety of repeated sessions of transcranial direct current stimulation: a systematic review. Brain Stimul 2018;11(2):278–88.
[5] O'Connell NE, Marston L, Spencer S, DeSouza LH, Wand BM. Non-invasive brain stimulation techniques for chronic pain. Cochrane Database Syst Rev 2018;4:CD008208.
[6] Gomes-Osman J, Indahlastari A, Fried PJ, Cabral DLF, Rice J, Nissim NR, et al. Non-invasive brain stimulation: probing intracortical circuits and improving cognition in the aging brain. Front Aging Neurosci 2018;10:177.
[7] Lefaucheur JP, Antal A, Ayache SS, Benninger DH, Brunelin J, Cogiamanian F, et al. Evidence-based guidelines on the therapeutic use of transcranial direct current stimulation (tDCS). Clin Neurophysiol 2017;128(1):56–92.
[8] Worsching J, Padberg F, Goerigk S, Heinz I, Bauer C, Plewnia C, et al. Testing assumptions on prefrontal transcranial direct current stimulation: comparison of electrode montages using multimodal fMRI. Brain Stimul 2018;11(5):998–1007.
[9] Dedoncker J, Brunoni AR, Baeken C, Vanderhasselt MA. A systematic review and meta-analysis of the effects of transcranial direct current stimulation (tDCS) over the dorsolateral prefrontal cortex in healthy and neuropsychiatric samples: influence of stimulation parameters. Brain Stimul 2016;9(4):501–17.
[10] Hill AT, Fitzgerald PB, Hoy KE. Effects of anodal transcranial direct current stimulation on working memory: a systematic review and meta-analysis of findings from healthy and neuropsychiatric populations. Brain Stimul 2016;9(2):197–208.
[11] Tremblay S, Lepage JF, Latulipe-Loiselle A, Fregni F, Pascual-Leone A, Theoret H. The uncertain outcome of prefrontal tDCS. Brain Stimul 2014;7(6):773–83.
[12] Minarik T, Berger B, Althaus L, Bader V, Biebl B, Brotzeller F, et al. The importance of sample size for reproducibility of tDCS effects. Front Hum Neurosci 2016;10:453.
[13] Vannorsdall TD, van Steenburgh JJ, Schretlen DJ, Jayatillake R, Skolasky RL, Gordon B. Reproducibility of tDCS results in a randomized trial: failure to replicate findings of tDCS-induced enhancement of verbal fluency. Cognit Behav Neurol 2016;29(1):11–7.
[14] Cattaneo Z, Pisoni A, Gallucci M, Papagno C. tDCS Effects on Verbal Fluency: a Response to Vannorsdall et al (2016). Cognit Behav Neurol 2016;29(3):117–21.
[15] Krause B, Cohen Kadosh R. Not all brains are created equal: the relevance of individual differences in responsiveness to transcranial electrical stimulation. Front Syst Neurosci 2014;8(25).
[16] Esmaeilpour Z, Marangolo P, Hampstead BM, Bestmann S, Galletta E, Knotkova H, et al. Incomplete evidence that increasing current intensity of tDCS boosts outcomes. Brain Stimul 2018;11(2):310–21.
[17] Bestmann S, Ward N. Are current flow models for transcranial electrical stimulation fit for purpose? Brain Stimul 2017;10(4):865–6.
[18] Jamil A, Batsikadze G, Kuo HI, Labruna L, Hasan A, Paulus W, et al. Systematic evaluation of the impact of stimulation intensity on neuroplastic after-effects induced by transcranial direct current stimulation. J Physiol 2017;595(4):1273–88.
[19] Indahlastari A, Chauhan M, Schwartz B, Sadleir RJ. Changing head model extent affects finite element predictions of transcranial direct current stimulation distributions. J Neural Eng 2016;13(6), 066006.
[20] Laakso I, et al. Inter-subject variability in electric fields of motor cortical tDCS. Brain Stimul 2015;8(5):906–13.
[21] Sadleir RJ, Vannorsdall TD, Schretlen DJ, Gordon B. Target optimization in transcranial direct current stimulation. Front Psychiatr 2012;3:90.
[22] Datta A, Truong D, Minhas P, Parra LC, Bikson M. Inter-individual variation during transcranial direct current stimulation and normalization of dose using MRI-derived computational models. Front Psychiatr 2012;3:91.
[23] Kasinadhuni AK, Indahlastari A, Chauhan M, Schar M, Mareci TH, Sadleir RJ. Imaging of current flow in the human head during transcranial electrical therapy. Brain Stimul 2017;10(4):764–72.
[24] Chauhan M, Indahlastari A, Kasinadhuni AK, Schär M, Mareci TH, Sadeir RJ. Low-frequency conductivity tensor imaging of the human head in vivo using DT-MREIT: first ftudy. IEEE Trans Med Imaging 2018;37(40):966–76.
[25] Huang Y, Liu AA, Lafon B, Friedman D, Dayan M, Wang X, et al. Measurements and models of electric fields in the in vivo human brain during transcranial electric stimulation. Elife 2017;6.
[26] Huang Y, Liu AA, Lafon B, Friedman D, Dayan M, Wang X, et al. Correction: measurements and models of electric fields in the in vivo human brain during transcranial electric stimulation. Elife 2018;7.
[27] Opitz A, Falchier A, Yan CG, Yeagle EM, Linn GS, Megevand P, et al. Spatiotemporal structure of intracranial electric fields induced by transcranial electric stimulation in humans and nonhuman primates. Sci Rep 2016;6:31236.
[28] Woods AJ, Bryant V, Sacchetti D, Gervits F, Hamilton R. Effects of electrode drift in transcranial direct current stimulation. Brain Stimul 2015;8(3):515–9.
[29] Opitz A, Paulus W, Will S, Antunes A, Thielscher A. Determinants of the electric field during transcranial direct current stimulation. Neuroimage 2015;109:140–50.
[30] De Witte S, Klooster D, Dedoncker J, Duprat R, Remue J, Baeken C. Left prefrontal neuronavigated electrode localization in tDCS: 10-20 EEG system versus MRI-guided neuronavigation. Psychiatry Res Neuroimaging 2018;274:1–6.
[31] Opitz A, Yeagle E, Thielscher A, Schroeder C, Mehta AD, Milham MP. On the importance of precise electrode placement for targeted transcranial electric stimulation. Neuroimage 2018;181:560–7.
[32] Woods AJ, Cohen R, Marsiske M, Alexander GE, Czaja SJ, Wu S. Augmenting cognitive training in older adults (The ACT Study): design and Methods of a Phase III tDCS and cognitive training trial. Contemp Clin Trials 2018;65:19–32.